Inorganic Chemistry

Article

pubs.acs.org/IC

Design Criteria for Polyazine Extractants To Separate An^{III} from Ln^{III}

Charles de Sahb,[†] Lori A. Watson,[‡] Janos Nadas,[†] and Benjamin P. Hay*[,†]

[†]Chemical Sciences Division, Oak Ridge National Laboratory, Oak Ridge, Tennessee 37831-6119, United States

[‡]Department of Chemistry, Earlham College, Richmond, Indiana 47374-4095, United States

Supporting Information

ABSTRACT: Although polyazine extractants have been extensively studied as agents for partitioning trivalent actinides from lanthanides, an explanation for why certain azine compositions succeed and others fail is lacking. To address this issue, density functional theory calculations were used to evaluate fundamental properties (intrinsic binding affinity for a representative trivalent f-block metal, basicity, and hardness) for prototype azine donors pyridine, pyridazine, pyrimidine, pyrazine, 1,2,3-triazine, 1,2,4-triazine, and 1,3,5-triazine, as well as perform conformational analyses of bisazine chelates formed by directly connecting two donors together. The results provide criteria that both rationalize the behavior of known extractants, TERPY, TPTZ, hemi-BTP, BTP, BTBP, and BTPhen, and predict a new class of extractants based on pyridazine donor groups.

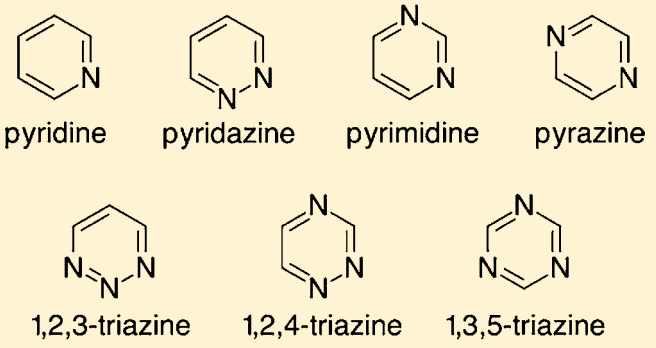

INTRODUCTION

Processing of spent nuclear fuel is an important aspect of the nuclear fuel cycle, allowing the recovery and reuse of uranium and plutonium, as well as minimizing the volume of nuclear waste.[1,2] In this context, a number of liquid−liquid extraction processes have been developed to effect various actinide separations from spent fuel.[2] One of the most challenging separations has proven to be the partitioning of trivalent actinides (An), Am^{3+} and Cm^{3+}, from lanthanides (Ln).[3−7] These two groups of metal ions are chemically similar, with both being hard Lewis acids with the same charge and similar ionic radii. Given the similarity in their properties, it was initially thought that An/Ln partitioning would be very difficult, if not impossible, to accomplish.[7]

The discovery[8] that ligands containing nitrogen donor groups exhibited a selectivity for An over Ln initiated an active field of research that continues to this day. Motivated by the observation that TERPY could selectively extract An from acidic aqueous solutions containing An and Ln, a large exploratory research effort focused on the attachment of various heterocyclic nitrogen donor groups to the 2 and 6 positions of a central pyridine donor to yield a series of tridentate extractants.[3−7] The current article focuses on a subset of these ligands, those obtained when six-membered ring heterocycles, in other words, azines, are used to construct the ligand. These extractants (Figure 1) have essentially the same architecture but differ in the identity of the donor group. Extension of this architectural motif has led to the tetraazines BTBP and BTPhen.

Prior reviews regarding these polyazine extractants[3−7] are largely descriptive in nature with an absence of discussion explaining why particular ligand compositions were selected for

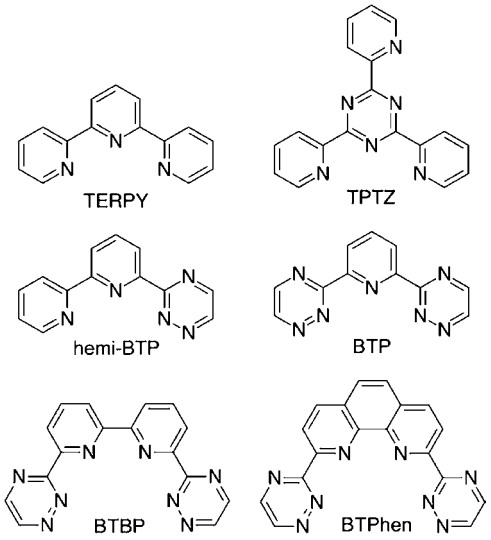

Figure 1. Polyazine extractants based on the TERPY architecture.

study over other possibilities. As a result, there is a lack of criteria with which to design alternative ligands that might exhibit improved extraction efficiency at low pH and enhanced An/Ln selectivity. Only three of seven possible azine, diazine, and triazine donors (see Figure 2) have been incorporated and tested within the TERPY architecture. Given that pyridine (**1**), pyrazine (**4**), and 1,3,5-triazine (**7**) could all occupy the central donor position, permutations of all seven azines in the terminal

Received: June 30, 2013
Published: August 23, 2013

   dx.doi.org/10.1021/ic401666m | *Inorg. Chem.* 2013, 52, 10632−10642

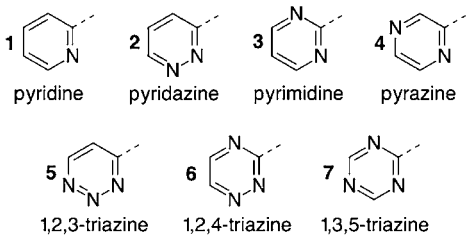

Figure 2. Prototype azine donor groups. The dashed line indicates the carbon atom to which an adjacent azine would be attached in the TERPY architecture.

positions give rise to 147 possible combinations, of which only 4 have been tested. Would any of the remaining 143 combinations yield extractants with enhanced An/Ln selectivity? Would variation of the donor composition enhance other desirable properties such as increased metal-ion affinity and decreased ligand basicity?

Herein, we address these questions by applying the concepts illustrated in Figure 3. That is to say, to a first approximation,

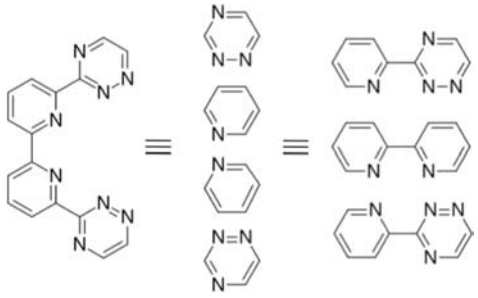

Figure 3. Multidentate ligands viewed as collections of both individual donor groups and bidentate chelates.

the properties of a multidentate ligand should reflect the properties of the individual donor groups within the ligand.[9] At the next level of approximation, structural effects present in a multidentate ligand can be rationalized by understanding the structural aspects associated with the individual chelate rings present within the ligand.[10] In what follows, electronic structure calculations are used to evaluate the intrinsic metal-ion affinity, pK_a, and hardness of the individual azines **1**− **7**, as well as the energetics of conformational reorganization in bisazine chelates. The results provide descriptors that rationalize the behavior of known extractants (Figure 1) and indicate the existence of a novel class of viable extractants based on pyridazine donor groups.

METHODS

Calculations were carried out with the *Gaussian 09* package[11] using density functional theory (DFT) at the B3LYP[12] level of theory. The LANL2DZ effective core potential basis set[13] was used for lanthanum, replacing 46 core electrons to account for scalar-relativistic effects. The 6-31+G* basis set was used for all carbon, nitrogen, and hydrogen atoms. Spin−orbit interactions were not considered explicitly. All reported structures were converged with the default self-consistent-field (tight) convergence cutoffs.[14] Minima for all unconstrained structures were confirmed by analytical calculation of the frequencies.

Using La^{3+} as a representative trivalent f-block metal ion, geometry optimizations were performed to locate the global minima for 1:1 complexes with azines **1**−**7**. To mimic the geometries observed in bisazine chelates, a second series of geometry optimizations were performed on these complexes, with one of the M−N−C angles constrained to position the metal ion along the vector from the azine centroid to the center of the coordinating nitrogen atom. For both series of complexes, metal-ion interaction energies, ΔE_1, were given by E(complex) − E(azine) − $E(La^{3+})$.

For evaluation of the metal complexation by bisazines, geometry optimizations were performed on the global minimum conformation of the ligand, the binding conformation of the ligand, and the La^{3+} complex. The structures of the binding conformations were obtained by geometry optimization, with the N−C−C−N dihedral angles between the azines constrained to 0.0°. Ligand reorganization energies going from the free to binding form, ΔE_{reorg}, were given by E(binding conformation) − E(free conformation). Lanthanum-ion interaction energies, ΔE_2, were given by E(complex) − E(binding conformation) − $E(La^{3+})$. The overall interaction energy, ΔE_{total}, which includes contributions from both reorganization and metal complexation, is given by E(complex) − E(free conformation) − $E(La^{3+})$, which is equivalent to ΔE_{reorg} + ΔE_2. An analogous approach was used to evaluate the energetics associated with trisazine ligands.

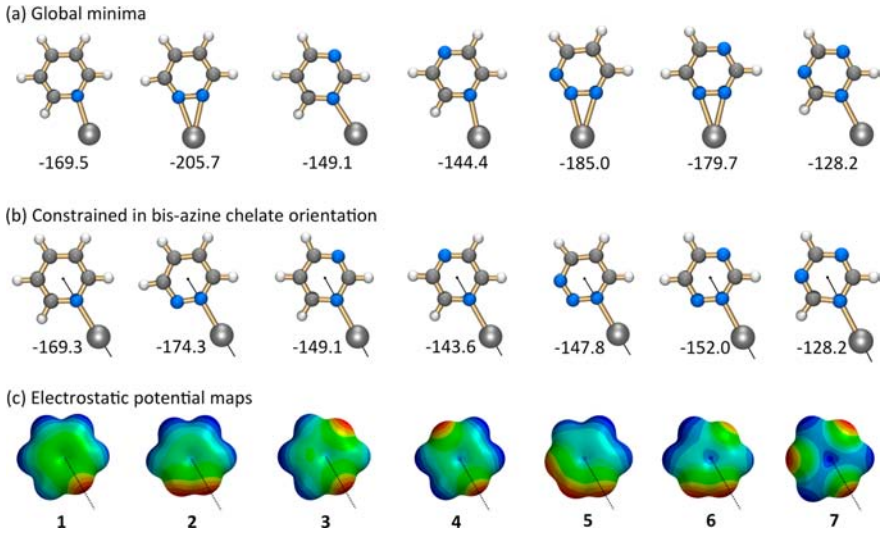

Figure 4. Optimized geometries and interaction energies (kcal/mol) for (a) global minima of La^{3+} complexes with **1**−**7** and (b) with the La−N−C angle constrained to approximate the La^{3+} location observed in bisazine chelate rings. (c) ESP mapped onto the electron density isosurface (0.002 e/Å^3) of the free azine ligand, with dotted lines showing the expected metal-ion location when in the bisazine chelate orientation.

dx.doi.org/10.1021/ic401666m | *Inorg. Chem.* 2013, 52, 10632−10642

Using the same level of theory, B3LYP/6-31+G*, further calculations were performed with *Spartan'10*.[15] The electrostatic potential (ESP) for each azine was mapped onto the 0.002 e/Å^3 electron density isosurface. Inspection of this map provided the value of the ESP, where the metal ion would contact the nitrogen atom in constrained 1:1 complexes. The hardness, η, of each azine was calculated as the difference between the ionization potential, IP, and electron affinity, EA. As described elsewhere,[16] these values were computed as IP = E(azine$^+$) − E(azine) and EA = E(azine) − E(azine$^-$), which correspond to the vertical IP and vertical EA from the bottom of the potential well of the neutral azine, respectively.

For the purpose of estimating unknown pK_a values, the energy difference for the following reaction was calculated for each azine: azine·H_2O + H_3O^+ → azine−H^+ + 2H_2O. Geometry optimization of each species at the B3LYP/6-31+G* level of theory and application of the SM8 model[17] to correct for aqueous solvation allowed the calculation of ΔE_{prot} = E(azine−H^+) + 2E(H_2O) − E(azine·H_2O) − E(H_3O^+). In cases where there was more than one possible protonation site, as in **5** and **6**, the lowest-energy form was used: N2 in **5** and N2 in **6**. The SM8 solvation model was also used to evaluate bisazine ΔE_{reorg} values in nonane, 1-octanol, and water.

RESULTS AND DISCUSSION

Properties of Isolated Azine Donors. Electronic structure calculations were used to evaluate several properties for isolated azine donor groups **1**−**7**. The first evaluation focused on the determination of the interaction energies for 1:1 complexes of a representative trivalent, f-block metal ion, La^{3+}, and azines in the gas phase, which are summarized in Figure 4a. The interaction energies cover a wide range from −205.7 to −128.2 kcal/mol. These results allow the azines to be ranked in order of their intrinsic metal-ion affinity. Going from strongest to weakest, the order is as follows: **2** > **6** > **5** > **1** > **3** > **4** > **7**. This ordering is fully consistent with experimental formation constants of azine adducts with the lanthanide metallocene complex $[Ce(C_5H_4R)_3]^0$ in an acetonitrile solvent: **2** (26) > **1** (8) > **3** (1) > **4** (0.4) > **7** (0.09), where 1:1 formation constant values are given in parentheses.[18]

The global minima geometries and interaction energies for the gas-phase complexes do not necessarily reflect the situation when these donors are incorporated in the bisazine chelate architecture exemplified by bipyridine, **1**-**1**. The location of the metal ion relative to each azine donor can be approximated by drawing a vector from the azine centroid through the center of the coordinated nitrogen atom, i.e., the one ortho to the carbon atom that would be bound to an adjacent azine. Optimized geometries and interaction energies, ΔE_1, for 1:1 azine−La^{3+} complexes constrained to this orientation are shown in Figure 4b and summarized in Table 1.

Upon comparison with the global minima (Figure 4a), it can be seen that the constrained structures are either (i) essentially unchanged, as with **3** and **7**, (ii) involve a displacement of the M−N−C angle, yielding an interaction energy that is destabilized by only a few tenths of a kilocalorie per mole, as with **1** and **4**, or (iii) exhibit a large change in the M−N−C angle as the interaction with two adjacent nitrogen donors changes to an interaction with a single nitrogen donor atom accompanied by a large destabilization ranging from 27 to 37 kcal/mol, as with **2**, **5**, and **6**. When constrained in the bisazine chelate orientation, the ranking from strongest to weakest changes to **2** > **1** > **6** > **3** > **5** > **4** > **7**, which differs from the relative order obtained using global minima only in the positions of **5** and **6**. The revised affinity order remains consistent with the available experimental data presented above.[18]

Table 1. Properties of Simple Azines[a]

azine	ΔE_1	ESP	pK_a	ΔE_{prot}	η
1	−169.3	−45.2	5.23	−17.96	10.83
2	−174.3	−47.0	2.33	−14.53	9.63
3	−149.1	−39.0	1.30	−12.72	10.37
4	−143.6	−37.3	0.65	−10.95	10.01
5	−147.8	−38.6	−0.54[b]	−6.00	9.94
6 (N2)	−152.0	−40.5	−0.16[b]	−7.92	9.33
6 (N4)	−124.2	−28.9			
7	−128.2	−32.5	−0.48[b]	−6.31	10.69

[a] ΔE_1 = E(azine·La^{3+}) − E(azine) − E(La^{3+}) in kilocalories per mole when constrained in the chelating orientation (Figure 4b); ESP = electrostatic potential where the metal contacts the nitrogen donor atom (kcal/mol); ΔE_{prot} = E(azine−H^+) + 2E(H_2O) − E(azine·H_2O) − E(H_3O^+) corrected for aqueous solvation using the SM8 model in kilocalories per mole; η = hardness in electronvolts. [b] Estimated from the correlation in Figure 6.

Given their classification as hard Lewis acids, the interaction between the trivalent f-block metal ions and organic bases is expected to be predominantly ionic in character.[9,19] Therefore, it should be possible to correlate the calculated affinities for La^{3+} with the magnitude of the ESP at the binding nitrogen atom. The ESP for each azine molecule was mapped onto the electron density isosurface at a value of 0.002 e/Å^3, which approximates the van der Waals surface of a molecule (Figure 4c). ESP values at the position on the nitrogen atom where the metal ion makes contact in the chelate orientation (Figure 4b) are given in Table 1. A plot of ESP versus ΔE_1 (Figure 5) shows that the La^{3+} binding affinity closely tracks the ESP, consistent with the concept that the lanthanum−nitrogen interaction is mostly ionic in character.

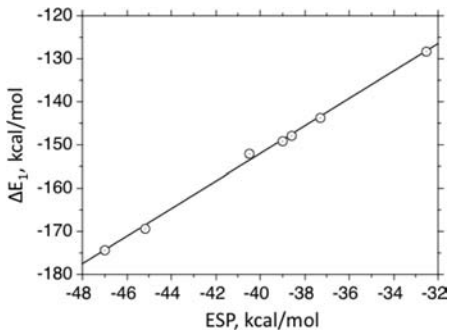

Figure 5. Plot of the La^{3+} interaction energy in the chelate orientation, ΔE_1 (Figure 4b), versus ESP on the free azine at the point where the metal ion would contact the nitrogen donor atom in the chelate orientation (Figure 4c). ΔE_1 = −24.27 + 3.194ESP, and r = 0.999.

Azine **6** is unique in that it offers two different donor atoms, either N2 or N4, when connected to another azine via C3. It has been noted that, in crystal structures of metal complexes with polyazine ligands such as BTP and BTBP (Figure 1), binding is always with N2; in other words, metal coordination with the N4 donor atom is never observed.[6] The preferred chelate binding orientation shown in Figure 4b is through N2. Consistent with the crystal structure evidence, the computed ΔE_1 = −124.2 kcal/mol for the N4 binding mode (not shown in Figure 4) is 27.8 kcal/mol weaker than that for the N2 binding mode. The reason for this energy difference is immediately apparent upon consideration of simple electro-

dx.doi.org/10.1021/ic401666m | *Inorg. Chem.* 2013, 52, 10632−10642

statics. The ESP for **6** exhibits a much weaker value at N4, −29.8 kcal/mol, than at N2, −40.9 kcal/mol.

Upon extraction of metal ions from acidic aqueous media, there is always the potential for ligand protonation to compete with metal-ion complexation. If the ligand is too basic, this competition can shut down the extraction. Therefore, azine basicity is an important property in the design of these extractants. Although experimental pK_a values have been measured for **1**−**4**[20] (see Table 1), such data are not available for the triazines **5**−**7**. Early estimates based on a dependence of known pK_a values with the local IP provide values of −1.77 for **6** and −2.31 for **7**.[21] A more recent study reports an estimated pK_a of −0.02 for **6** from a dependence of known pK_a values with calculated gas-phase protonation energies.[22]

Given the significant discrepancy in the prior estimates for **6**, further calculations were performed here. Figure 6 shows a plot

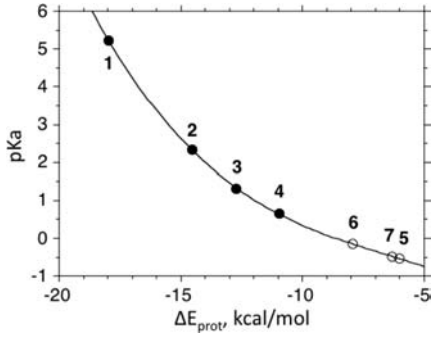

Figure 6. Dependence of pK_a versus ΔE_{prot} allowing an estimate of pK_a values for **5**−**7**.

of pK_a versus ΔE_{prot}, the solvation-corrected energy difference for the reaction: azine·H_2O + H_3O^+ → azine−H^+ + 2H_2O. Extrapolation of the dependence in Figure 6 yields pK_a estimates of −0.54 for **5**, −0.16 for **6**, and −0.48 for **7**. It should be noted that the azine pK_a, which measures the strength of the covalent bond with a proton, is poorly correlated with ΔE_1, which measures the strength of the electrostatic interaction with La^{3+}. Taking values from Table 1, a plot of ΔE_1 versus pK_a (not shown) demonstrates a distinct lack of correlation between these two properties.

A final property of interest is the hardness of the azine. Selectivity for An^{3+} over Ln^{3+} has been rationalized by the presence of a minor covalent contribution in the metal−nitrogen interaction that is slightly stronger with An than with Ln.[3−7] It has been suggested that differences in the selectivity exhibited by different azines can be predicted by a computable property known as the hardness, η, defined as the difference in energy between the IP and EA.[23] Computed η values for **1**−**7** (Table 1) yield the following ranking for the softest to hardest azine: **6** < **2** < **5** < **4** < **3** < **7** < **1**.

Experimental data on the An/Ln selectivity for the prototype azine ligands, **1**−**7**, are limited to one study.[18] The concept that η predicts changes in the selectivity exhibited by single azine donors is consistent with the observation that U^{3+}/Ce^{3+} selectivity increased from 3.0 to 4.2 on going from the harder **1** to the softer **3**. In another example, involving an ethylenediaminetetraacetic acid analogue in which two of the carboxyl groups are replaced with azine donors, it was observed that changing the identity of the azines from the harder **1** to the softer **4** increased Am^{3+}/Eu^{3+} selectivity by a factor of 8.[23]

La^{3+} Chelates with Bisazines. A total of 28 unique bisazine ligands were constructed by combining every possible azine pair using **1** through **7**. Geometry optimizations of the La^{3+} complexes with these bisazines all yielded planar minima, with the metal forming a five-membered chelate ring, as shown in Figure 7a. In the case of bipyridine, **1**-**1**, the calculated

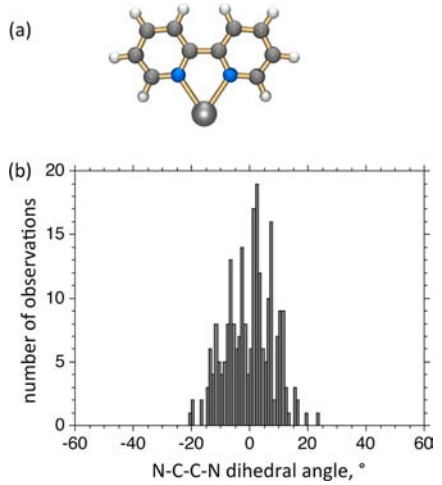

Figure 7. (a) **1**-**1** complex with La^{3+} provides a representative example of the bisazine chelate geometry. (b) Distribution of N−C−C−N dihedral angles in crystal structures of **1**-**1** complexes with all Ln^{3+} metal ions consistent with a weak preference for planarity (r_{fac} < 0.10, no error, no disorder, and no powder structures).

geometry can be compared with numerous examples from the Cambridge Structural Database (CSD)[24] that have been reported for all Ln^{3+} complexes. These structures exhibit the following average features: Ln−N distance of 2.59 ± 0.08 Å, inner Ln−N−C angle of 121.5 ± 1.6° (calcd 120.4°), outer Ln−N−C angle of 120.2 ± 1.7° (calcd 119.8°), and an N−C−C−N dihedral angle distribution (Figure 7b), consistent with a planar geometry preference. Consistent with expected trends in the metal−ligand distance as a function of the coordination number,[25] the calculated La−N distance of 2.401 Å at CN = 2 is significantly shorter than the La−N distance of 2.70 ± 0.05 Å observed in crystal structures at CN ≥ 9.

Bisazine chelate rings are expected to exhibit a metal-ion size preference, with the most stable complex occurring at the M−N distance that yields strain-free M−N−C angles.[10b] With **1**-**1**, this situation occurs at a M−N distance of 2.49 Å, which falls within the range of values observed in the CSD for the trivalent lanthanides, 2.45−2.70 Å. The optimal M−N distances for other bisazine chelates also fall within this range. It should be noted that relatively small distortions in the M−N−C angles, ≤2°, are needed to accommodate all members of the An and Ln series; in other words, the energetic penalty arising from metal size mismatch in bisazine chelate rings is expected to be small for the range of sizes encountered within the trivalent f-block metal ions. Further information regarding the geometric aspects of polypyridine metal complexes is provided in a recent review.[26]

In the majority of the cases, the planar bound form of the bisazine is not a stable conformation in the absence of the metal ion. To separate the energetic contributions arising from ligand conformational reorganization from those arising from intrinsic metal-ion affinity, the metal complexation can be divided into a two-step process: (i) ligand reorganization from the global

dx.doi.org/10.1021/ic401666m | Inorg. Chem. 2013, 52, 10632−10642

minimum conformation to the planar binding conformation followed by (ii) metal-ion binding to this ligand conformation (Figure 8). The energy change for the first step, ΔE_{reorg}, must

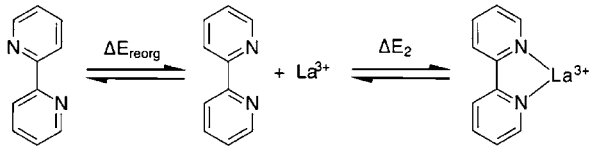

Figure 8. Energetics of metal-ion complexation by bisazine chelates, such as **1-1**, can be separated into a contribution from ligand reorganization, ΔE_{reorg}, and a contribution from metal–ligand binding, ΔE_2.

be added to the La^{3+} interaction energy, ΔE_2, to obtain the effective interaction energy, ΔE_{total}. In other words, $\Delta E_{total} = E(\text{complex}) - E(\text{free ligand}) = \Delta E_{reorg} + \Delta E_2$. Conformational analysis and ΔE_{reorg} values are presented in the next section.

Interaction energies obtained when La^{3+} coordinates with the planar binding conformation, ΔE_2, are summarized in Table 2.

Table 2. La^{III} Interaction Energies, ΔE_2 (kcal/mol), for Complexation of Bisazine Ligands Constrained in Their Planar Binding Configuration

bisazine	ΔE_2	bisazine	ΔE_2
1-1	−266.5	**3-4**	−230.9
1-2	−275.5	**3-5**	−238.0
1-3	−253.4	**3-6**	−242.7
1-4	−244.7	**3-7**	−220.8
1-5	−253.3	**4-4**	−222.3
1-6	−256.7	**4-5**	−232.4
1-7	−234.8	**4-6**	−235.2
2-2	−279.0	**4-7**	−212.2
2-3	−260.6	**5-5**	−236.6
2-4	−254.8	**5-6**	−238.5
2-5	−257.5	**5-7**	−219.2
2-6	−260.4	**6-6**	−243.7
2-7	−241.8	**6-7**	−223.5
3-3	−239.8	**7-7**	−201.7

As with the single azine donors, the ΔE_2 values exhibit a wide range of values, going from the weakest interaction with **7-7**, −201.7 kcal/mol, to the strongest interaction with **2-2**, −279.0 kcal/mol. The magnitude of the ΔE_2 values for the bisazines can be predicted using the intrinsic binding affinities of the individual azine donors, ΔE_1 (Table 1). A plot of ΔE_2 versus the sum of ΔE_1 for each azine in the chelate gives the linear correlation shown in Figure 9, which establishes that the La^{3+} interaction energy with a bisazine is approximately 80% of the $\sum\Delta E_1$ value. This result provides an example of how the properties of a multidentate ligand can be predicted from the properties of the components.

Conformational Properties of Bisazines. Structural reorganization in this series of bisazines is due to rotation about the C–C bond connecting the two azines. The lowest-energy rotamer for each bisazine was identified by evaluation of the C–C rotational potential energy surface. The energy change on going from the lowest-energy form to the planar binding form, ΔE_{reorg}, was computed for all 28 bisazines in the gas phase, nonane, 1-octanol, and water; see Table 3.

Depending on the number of *o*-hydrogen atoms, three distinct types of behavior are observed, as depicted by the

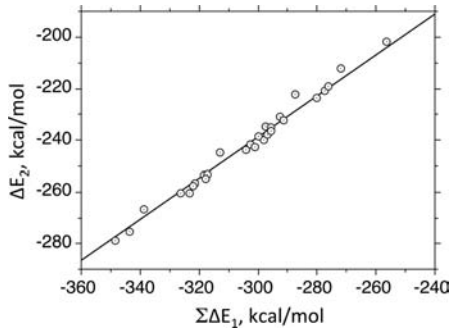

Figure 9. Correlation between the La^{3+} interaction energy with the bisazines constrained in the planar binding conformation, ΔE_2 (Table 2), and the sum of the La^{3+} interaction energies with individual azines present in the bisazines, $\sum\Delta E_1$ (see Table 1 for ΔE_1 values). $\Delta E_2 = 0.796\sum\Delta E_1$, and $r = 0.992$.

Table 3. Energy Change, ΔE_{reorg} (kcal/mol), on Going from the Global Minimum Conformation with an Azine–Azine Twist Angle of ϕ to the Planar Binding Conformation

		ΔE_{reorg}			
bisazine	ϕ at minimum	gas phase	nonane	1-octanol	water
1-1	0.0	7.6	7.3	6.3	5.8
1-2	0.0	8.8	8.2	6.6	6.0
1-3	0.3	0.0	0.0	0.0	0.0
1-4	0.0	6.7	6.3	5.3	4.9
1-5	0.0	8.4	7.8	6.2	5.5
1-6	0.3	1.1	0.7	0.1	0.0
1-7	0.6	0.0	0.0	0.0	0.0
2-2	0.0	10.4	9.4	7.2	6.4
2-3	4.9	0.0	0.0	0.0	0.0
2-4	0.0	7.6	6.9	5.5	5.0
2-5	0.0	10.0	8.9	6.5	5.7
2-6	9.7	1.5	1.1	0.3	0.2
2-7	6.4	0.0	0.0	0.0	0.0
3-3	39.5	0.6	0.5	1.3	1.7
3-4	5.1	0.1	0.0	0.0	0.0
3-5	1.0	0.0	0.0	0.0	0.0
3-6	43.0	0.7	0.5	1.2	1.7
3-7	37.5	0.4	0.3	0.8	1.2
4-4	0.0	6.0	5.4	4.5	4.1
4-5	0.0	7.3	6.3	4.6	4.0
4-6	5.5	0.9	0.6	0.1	0.0
4-7	0.1	0.0	0.0	0.0	0.0
5-5	0.0	9.6	8.4	5.9	5.0
5-6	10.0	1.5	1.0	0.2	0.0
5-7	3.0	0.0	0.0	0.0	0.0
6-6	42.7	1.3	1.1	1.7	2.0
6-7	39.6	0.6	0.3	0.9	1.2
7-7	37.6	0.4	0.1	0.6	0.9

rotational potential energy surfaces shown in Figure 10. When there are two *o*-hydrogen atoms, as illustrated by **1-1** in Figure 10 (top), the global minimum is planar, with the two donor nitrogen atoms in a trans arrangement. This behavior is exhibited when both donors of the bisazine are from the set {**1**, **2**, **4**, **5**}. Such structures exhibit large gas-phase reorganization energies, 6.7–10.4 kcal/mol, on going from this trans form to the planar cis binding form, which is a transition state on the rotational potential surface. On moving from the gas phase to progressively more polar environments, in other words,

dx.doi.org/10.1021/ic401666m | *Inorg. Chem.* 2013, 52, 10632–10642

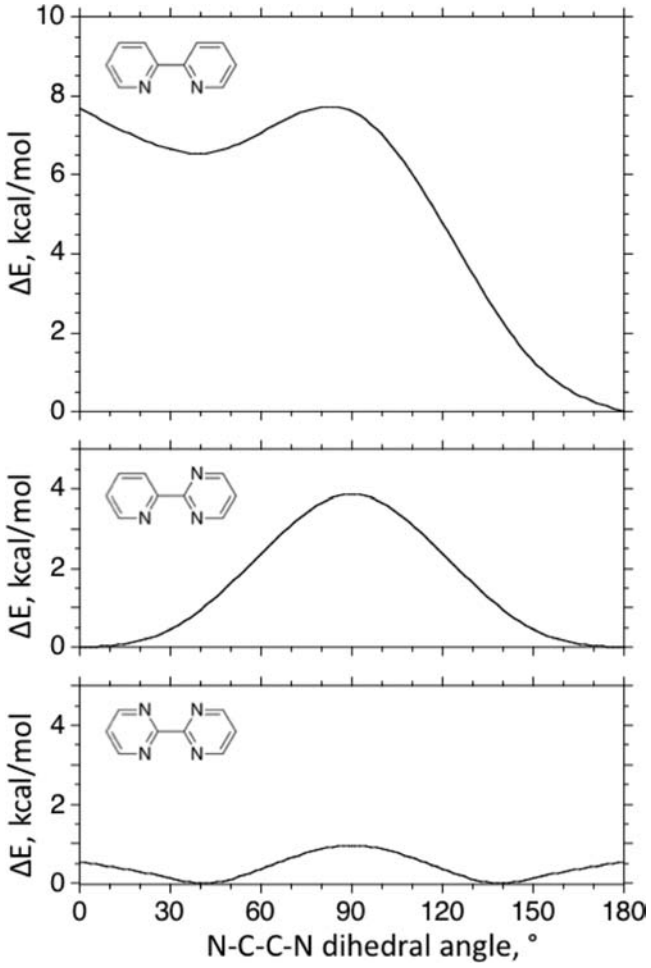

Figure 10. Representative rotational potential energy surfaces for the three types of behavior: (top) two *o*-hydrogen atoms; (middle) one *o*-hydrogen atom; (bottom) no *o*-hydrogen atoms.

nonane, 1-octanol, and water, continuum solvent models predict that the ΔE_{reorg} values become progressively weaker, with an average decrease to 64% of the gas-phase value (Table 3).

When there is only one *o*-hydrogen atom, as illustrated by **1**-**3** in Figure 10 (middle), the global minimum is either planar or nearly planar. This behavior is exhibited when the bisazine contains one donor from the set {**1**, **2**, **4**, **5**} and the other donor from the set {**3**, **6**, **7**}. When **3** and **7** are present, the two planar minima are identical and the lowest-energy form is the binding conformation; in other words, ΔE_{reorg} = 0 kcal/mol. When **6** is present, the behavior is slightly altered because of the previously discussed differences between N2 and N4. Relative to the other azine nitrogen donor, N2 is trans in the global minimum and cis in the binding conformation. Thus, reorganization is required for metal chelation, but gas-phase ΔE_{reorg} values are small, ranging from 0.9 to 1.5 kcal/mol.

When there are no *o*-hydrogen atoms, as illustrated by **3**-**3** in Figure 10 (bottom), the global minima are not planar and the two azines twist 37−43° with respect to one another. This behavior is exhibited when both donors of the bisazine are from the set {**3**, **6**, **7**}. However, the energy to organize the ligand into the planar binding conformation is again small, with gas-phase ΔE_{reorg} values ranging from 0.4 to 1.3 kcal/mol.

The ΔE_{reorg} values observed with the first group of bisazines represented by **1**-**1** have been attributed to unfavorable van der Waals interactions between the two hydrogen atoms when the ligand is forced into the cis form.[26] To evaluate the validity of this hypothesis, single-point-energy calculations were performed with a MM3 force field[27] on the DFT geometry of the cis and trans forms of **1**-**1**. The molecular-mechanics output allows inspection of the van der Waals energy for each atom-pair interaction. As shown in Figure 11, there are four close

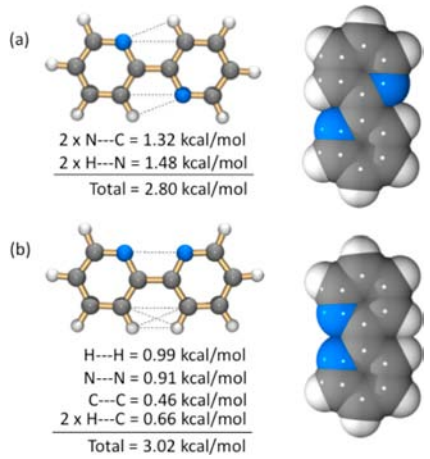

Figure 11. MM3 van der Waals energies for close interazine contacts in B3LYP/6-31+G* geometries of **1**-**1** in the (a) trans and (b) cis conformations.

contacts in the trans form and five close contacts in the cis form. Summing the van der Waals contributions from these contacts reveals that, although the H---H contact in the cis form does contribute a 0.99 kcal/mol destabilizing contribution, when the contributions from all close contacts are taken into account, the difference in van der Waals repulsion between the cis and trans forms is only 0.22 kcal/mol. Thus, the large ΔE_{reorg} value is not explained by unfavorable interazine van der Waals interactions.

An alternate explanation for large ΔE_{reorg} values when two *o*-hydrogen atoms are present could be an unfavorable electrostatic interaction between the two nitrogen donor atoms when they are forced into contact in the cis conformation. However, this explanation is inconsistent with the rotational potential surfaces for bisazines containing no *o*-hydrogen atoms (Figure 10, bottom). Here when the twisted global minima are forced into a planar configuration bringing two pairs of nitrogen atoms into close contact, examination of Table 3 shows that the energy increase never exceeds 1.3 kcal/mol.

Further consideration of the rotational potential surface for **1**-**1** offers a third explanation. Using the 90° N−C−C−N dihedral angle structure as a reference point, the change in energy on going to the 0° cis form is only +0.1 kcal/mol, whereas the change on going to the 180° trans form is −7.5 kcal/mol. Thus, the difference in energy between the cis and trans forms is not due to destabilization of the cis form but a rather large stabilization of the trans form. This stabilization can be explained if it is assumed that each of the two C−H---N contacts present in the trans form represents energetically favorable interactions as recently suggested.[28] The formation of stabilizing C−H---N interactions also accounts for the observation of planar global minima when only one *o*-hydrogen atom is present. On going from the 90° form of **1**-**3** to the

dx.doi.org/10.1021/ic401666m | *Inorg. Chem.* 2013, 52, 10632−10642

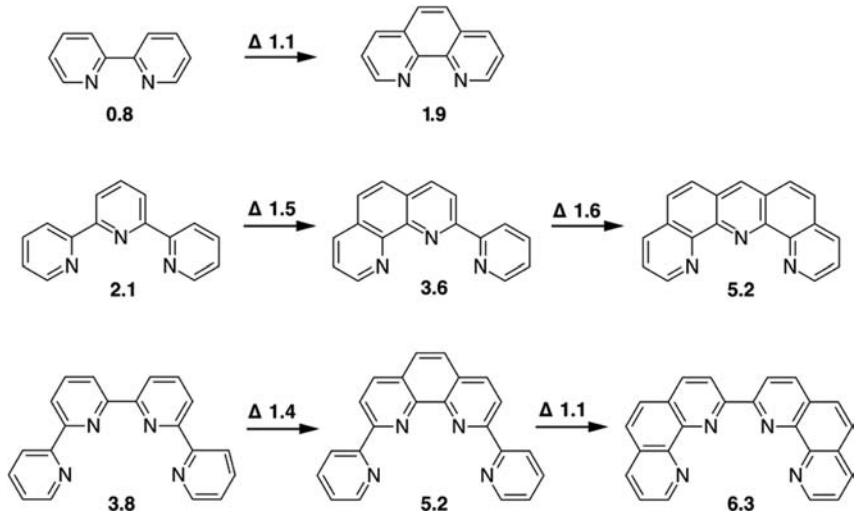

Figure 12. Influence of preorganization in the polypyridyl ligands on the binding affinity illustrated by a change in the log K values for La^{III} complexation in water or a water/methanol solution.[31].

planar 0° form, the energy drops by −3.9 kcal/mol (one C−H---N interaction), roughly half the −7.5 kcal/mol drop in **1-1** (two C−H---N interactions). Finally, the absence of stabilizing C−H---N interactions is consistent with the twisted conformations observed in the absence of *o*-hydrogen atoms and the small energy change, <0.5 kcal/mol, on going from the 90° form of **3-3** to the planar 0° form.

Influence of Preorganization. Metal−ligand interactions are maximized when the ligand is constrained in the binding conformation, in other words, when the ligand is preorganized.[29] When preorganized, ΔE_{reorg} = 0 kcal/mol. This can be achieved in bisazines by adding an additional bridge between the two azines. A classic example is provided by phenanthroline (Figure 12), which is a preorganized version of **1-1**. A comparison of aqueous log K values for first-row transition-metal ions shows that this preorganization results in an average increase in the binding affinity by 1.4 log units, which corresponds to an energy difference of 1.9 kcal/mol at 25 °C.[30] Similar binding affinity enhancements have been reported for La^{3+} with the series of ligands presented in Figure 12, where the replacement of **1-1** with phenanthroline increases binding by 1.1−1.6 log units in protic solvents such as water and a water/methanol mixture.[31]

Experimental enhancement upon preorganization of the **1-1** chelate to the phenanthroline analogue, 1.9 kcal/mol, is smaller than that predicted when the gas-phase value is corrected for aqueous solvation, 5.8 kcal/mol (Table 1). One explanation for the discrepancy is that the intrinsic binding affinity of phenanthroline could be weaker than that of **1-1**. To test this hypothesis, the gas-phase interaction energy for La^{3+} with phenanthroline was calculated. Rather than being a weaker donor, phenanthroline exhibits a ΔE_2 value of −278.6 kcal/mol, 4.5% stronger than that for **1-1**. This result establishes that **1** becomes an intrinsically stronger donor group when two of these azines are conjugated to a central arene core and not a weaker one.

Although the SM8 solvation model applied in this study correctly predicts that the ΔE_{reorg} value for **1-1** will decrease on going from the gas phase to the aqueous solution, it underestimates the magnitude of the decrease. It can be argued that specific solvent interactions, such as hydrogen bonding between water molecules and the azine nitrogen atoms, would act to disrupt the stabilizing intramolecular C−H---N interactions responsible for the large ΔE_{reorg} values, thereby significantly reducing the cost of structural reorganization. This result suggests that it may be necessary to evaluate the rotational potential surfaces of bisazines with two or more solvent molecules present in order to achieve more accurate results in hydrogen-bonding solvents.

Putting the Pieces Together: Polyazine Ligands. Given the properties of individual azines and the conformational characteristics of bisazine ligands, to what extent is it possible to rationalize the behavior of polyazine ligands? Using an approach analogous to that depicted in Figure 8, La^{3+} interaction energies with the planar binding conformation, ΔE_3, and conformational reorganization energies, ΔE_{reorg}, were calculated for several trisazine ligands, including those representative of known extractants TERPY (**1-1-1**), hemi-BPT (**1-1-6**), BTP (**6-1-6**), and TPTZ (**1-7-1**), as well as some novel trisazine compositions containing **2**.

The energetic results are summarized in Table 4. As with the bisazines, the calculated intrinsic binding affinities, ΔE_3, are correlated with the sum of the binding affinities for each azine component, ΔE_1 (Table 1). A plot of ΔE_3 versus $\sum\Delta E_1$ gives

Table 4. Predicted Properties of Selected Trisazine Chelates[a]

trisazine	ΔE_3	ΔE_{reorg}	ΔE_{total}	ave pK_a	ave η
1-1-1, TERPY	−354.4	15.5	−338.9	5.23	10.83
1-1-6, hemi-BTP	−346.7	9.8	−337.1	3.42	10.33
6-1-6, BTP	−338.7	2.8	−335.9	1.61	9.83
1-7-1	−329.8	0.0	−329.8	3.30	10.78
2-1-2	−367.8	18.0	−349.8	3.30	10.03
2-1-2, p	−367.6	0.0	−367.6	3.30	10.03
2-4-2	−349.4	15.7	−333.7	1.77	9.76
2-4-2, p	−349.0	0.0	−349.0	1.77	9.76
2-7-2	−338.5	0.2	−338.3	1.36	9.98

[a]Energies reported in kilocalories per mole and η in electronvolts. ΔE_3 = E(complex) − E(ligand in binding form) − $E(La^{3+})$; ΔE_{reorg} = E(ligand in binding form) − E(ligand in global minimum form); $\Delta E_{total} = \Delta E_3 + \Delta E_{reorg}$. Average p$K_a$ and η values are defined as the sum of the corresponding values for individual azines (Table 1) divided by the number of azines in the ligand.

dx.doi.org/10.1021/ic401666m | *Inorg. Chem.* 2013, 52, 10632−10642

the linear correlation shown in Figure 13, which establishes that the La^{3+} interaction energy with a trisazine is approximately 71% of the $\sum\Delta E_1$ value. This result provides a second example of how the properties of a multidentate ligand can be predicted from the properties of the components.

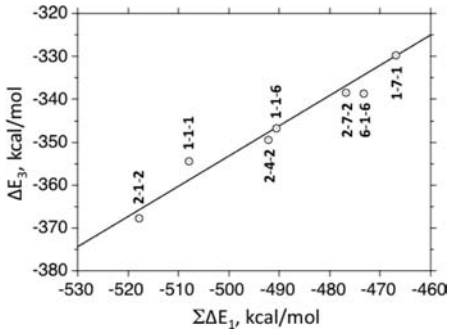

Figure 13. Correlation between the La^{3+} interaction energy with trisazines constrained in the planar binding conformation, ΔE_3 (Table 4), and the sum of the La^{3+} interaction energies with individual azines present in the trisazines, $\sum\Delta E_1$ (see Table 1 for ΔE_1 values). $\Delta E_3 = 0.706\sum\Delta E_1$, and $r = 0.976$.

This correlation provides insight into why known trisazine extractants perform as well as they do. Azine components **1** and **6** have the second and third strongest ΔE_1 values. Thus, **1**-**1**-**1**, **1**-**1**-**6**, and **6**-**1**-**6** represent compositions that provide some of the strongest possible intrinsic metal-ion affinities obtainable using this ligand architecture. Although **1**-**7**-**1** contains two of the stronger azines, it also contains the weakest azine **7**. As a result, **1**-**7**-**1** presents the weakest intrinsic metal-ion affinity of this series.

Azine **2** exhibits the largest ΔE_1 value (Table 1). Two of these azines can be connected to either **1**, **4**, or **7** to give novel trisazine compositions. The **2**-**1**-**2** composition represents the highest possible intrinsic metal-ion affinity for a trisazine with the TERPY architecture. The other two compositions, **2**-**4**-**2** and **2**-**7**-**2**, exhibit ΔE_3 values that are as strong or stronger than that of **6**-**1**-**6**.

The overall binding affinity, ΔE_{total}, is given by the sum of ΔE_3 plus the cost of structural reorganization, ΔE_{reorg}. The trisazines contain two rotatable bonds. As shown in Figure 14, the ΔE_{reorg} value for a trisazine ligand can be predicted to be

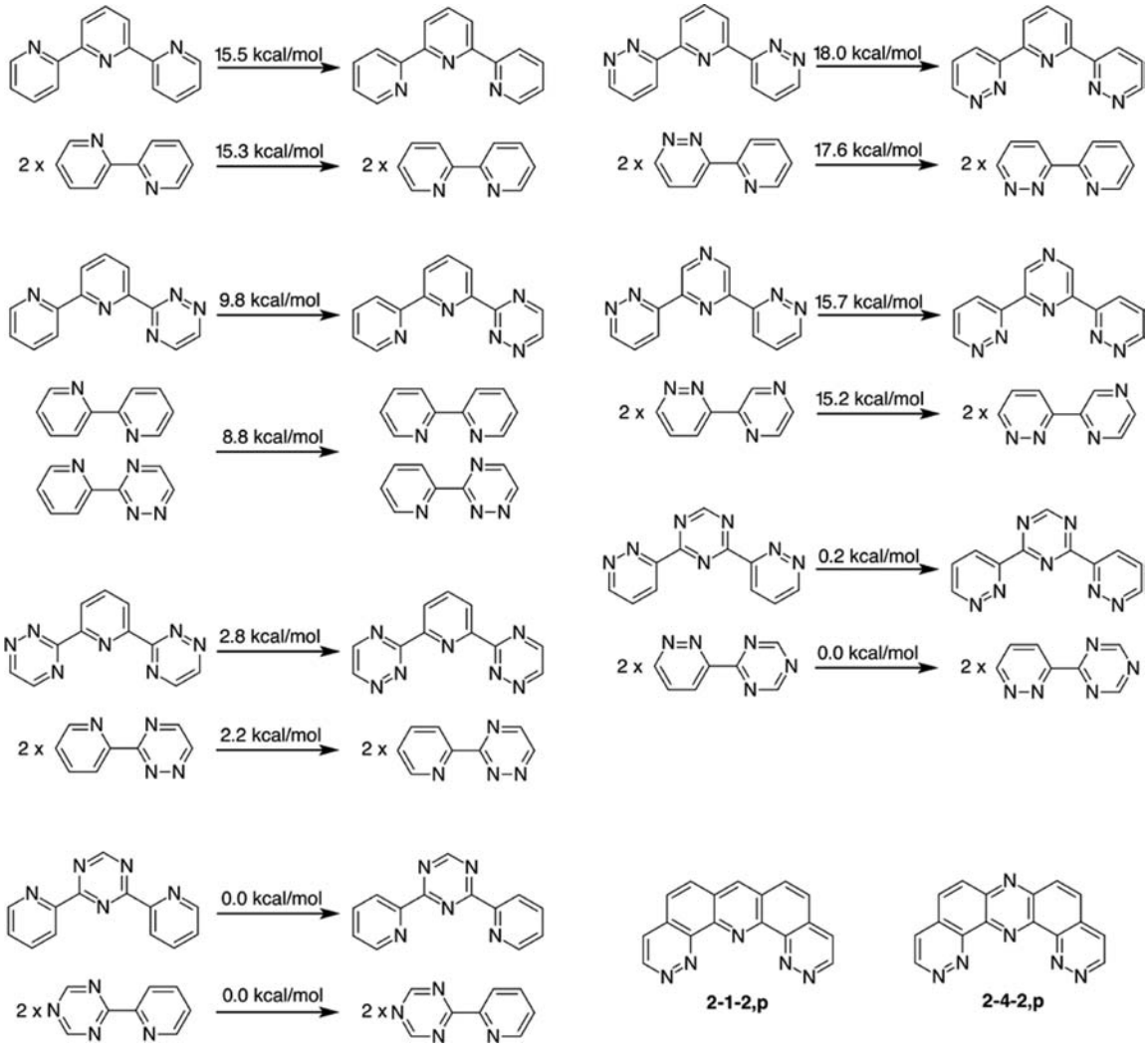

Figure 14. Examples showing how ΔE_{reorg} for trisazine ligands can be predicted to within 1 kcal/mol by summing the ΔE_{reorg} values associated with each rotatable bond in the analogous bisazine ligand (Table 3).

dx.doi.org/10.1021/ic401666m | Inorg. Chem. 2013, 52, 10632−10642

within 1 kcal/mol by summing the ΔE_{reorg} values associated with each rotatable bond in the corresponding bisazines (Table 3). For the known extractants, the magnitudes of the ΔE_{reorg} values are inversely correlated with the ΔE_3 values, such that the two components act to offset one another to give a relatively constant ΔE_{total}, −335.9 to −338.9 kcal/mol, for **1**-**1**-**1**, **1**-**1**-**6**, and **6**-**1**-**6**. This indicates that observed log *K* values should be relatively constant over this series. Even though the trisazine corresponding to TPTZ, **1**-**7**-**1**, has the lowest ΔE_{reorg}, 0 kcal/mol, the low ΔE_3 value gives the weakest ΔE_{total}, −329.8 kcal/mol, for the known trisazine extractants. Experimental log *K* values reveal that these trisazines all form 1:1 La^{3+} complexes of similar stability in protic solvents: TPTZ, 1.95 (H_2O);[26] TERPY, 2.08 (H_2O);[26] BTP, 2.20 (75% MeOH/H_2O).[6]

Conformational analysis of trisazines containing **2** reveals that even with the highest ΔE_{reorg} value in Table 4, **2**-**1**-**2** forms the strongest possible complex, ΔE_{total} = −349.8 kcal/mol, for this trisazine architecture. The other two compounds, **2**-**4**-**2** and **2**-**7**-**2**, give ΔE_{total} values within the range of values for the known extractants. In addition to its high metal-ion affinity, **2** can be fused to the central azine to yield a preorganized architecture. The resulting structures, **2**-**1**-**2**,p and **2**-**4**-**2**,p (Figure 14), exhibit the strongest possible La^{3+} binding, ΔE_{total} = −367.6 and −349.0 kcal/mol, respectively, that can be obtained when three simple azines are connected in this fashion.

The influence of preorganization was recently demonstrated when one of the three rotatable bonds in the tetraazine extractant, BTBP, was constrained in BTPhen (Figure 1). This modification yielded a stronger extractant with a 100-fold increase in the metal distribution coefficient for partitioning into 1-octanol from an aqueous solution.[32] The magnitude of this increase, which corresponds to an energy difference of 2.6 kcal/mol at 25 °C, is only slightly higher than that observed for the formation of 1:1 La^{3+} complexes with polypyridyl ligands in an aqueous or a water/methanol solvent (see Figure 12). Recent thermodynamic studies in acetonitrile suggest that BTPhen does form a stronger 2:1 complex with La^{3+} than BTBP, although it was not possible to quantify the magnitude of the enhancement.[33]

In addition to possessing sufficient metal binding affinity to form stable complexes in the organic phase, ligands for An/Ln separation must be able to extract these metal ions from nitric acid solutions at low pH.[3−7] Thus, low ligand basicity is a desirable property. Given the possibility of multiple conformations and protonation sites in polyazines, calculation of the pK_a or values that might correlate with pK_a, such as the ΔE_{prot} value presented above, is not a simple process. As an alternative quick approximation, one can use the average pK_a of the ligand donors as a gauge of the basicity in a polyazine. This value, which is computed by summing the pK_a for each donor group and dividing by the number of donor groups, is given in Table 4.

A comparison with available experimental pK_a values for trisazines in an aqueous solution[30] suggests that the ave pK_a descriptor gives reasonable estimates for TERPY (exp 4.65, est 5.23) and TPTZ (exp 3.53, est 3.30). The replacement of strongly basic pyridine donors, **1**, with acidic triazines, **6** or **7**, should result in less basic ligands. This concept inspired the design of TPTZ.[3] In liquid−liquid extraction experiments, trisazine extractants function at increasingly lower pH as the triazine content increases: BTP (**6**-**1**-**6**) < TPTZ (**1**-**7**-**1**) ∼ hemi-BTP (**1**-**1**-**6**) < TERPY (**1**-**1**-**1**).[7] This trend is consistent with the decreasing basicity predicted by the average pK_a values.

Average pK_a values for the proposed trisazines containing **2** range from a high of 3.30 to a low of 1.36. The most basic of these ligands, **2**-**1**-**2**, has a ave pK_a similar to those of **1**-**1**-**6** and **1**-**7**-**1**; however, the enhanced metal-ion affinity associated with **2**-**1**-**2** may prove sufficient to compete with protonation, allowing use at lower pH than can be reached with the known extractants. A similar comment applies to **2**-**4**-**2**, which has an ave pK_a similar to that of **6**-**1**-**6** but a stronger metal-ion affinity. Finally, **2**-**7**-**2** is estimated to be the least basic of all high-metal-ion-affinity trisazines summarized in Table 4.

In addition to the ability to form extractable complexes in the presence of competing protonation, a viable ligand must exhibit sufficient An/Ln selectivity. Experimental S_{fac}(Am/Eu) values with polyazine extractants generally range from 10 to 1000,[3] which corresponds to energy differences of 1.36−4.08 kcal/mol at 25 °C. The magnitude of the effect is small relative to the intrinsic metal interaction energies. In the case of BTP, which forms 3:1 complexes containing a total of nine metal−nitrogen interactions, an S_{fac}(Am/Eu) of 1000 corresponds to an average increase in energy of only 0.45 kcal/mol/bond on going from Eu^{3+} to Am^{3+}. In the case of BTBP, which forms 2:1 complexes containing eight metal−nitrogen interactions, an S_{fac}(Am/Eu) of 100 corresponds to an even smaller increase in energy of 0.34 kcal/mol/bond.

Such small differences in the interaction energy have been attributed to the fact that, although these metal−ligand interactions are predominantly ionic in character, there exists a small covalent component that is slightly larger with actinides than with lanthanides.[19] Much theoretical effort has been expended in an attempt to characterize the nature of this covalent contribution. As noted in a recent comprehensive review of this effort,[34] although such calculations sometimes provide evidence for increased covalency in An^{III} complexes, in most cases, An^{III} interaction energies are predicted to be lower than their Ln^{III} counterparts. In other words, in most cases, electronic structure models predict that polyazines have a stronger affinity for Ln^{III} rather than An^{III}. Given that this trend is opposite to experimental observation, one conclusion could be that current DFT methods and/or basis sets have not yet reached a sufficient level of accuracy to allow a reliable prediction of the magnitude of the small covalent contributions that are present in these systems.

Given these difficulties, no attempts were made to compute differences in the interaction energy for An/Ln couples with **1**−**7** or any of the polyazines containing these donor groups. Instead, electronic structure calculations were used to compute the hardness of the azine donors, with the concept that the An/Ln selectivity would correlate with this azine descriptor. As discussed earlier, this concept is supported by a comparison of the experimental log *K* data in a couple instances.[18,23] If η correlates with An/Ln selectivity, then one can propose that the average η value in a polyazine should provide a descriptor that correlates with the observed selectivity. A review tracing the evolution of polyazine extractant development provides maximum S_{fac}(Am/Eu) values that had been observed for the following ligands: TERPY, 10; TPTZ, 10; hemi-BTP, 30; BTBP, 100; BTP, 1000.[3] A plot of log S_{fac}(Am/Eu) versus ave η; in other words, the sum of η values for each donor (Table 1) divided by the number of donors reveals the relationship shown in Figure 15.

dx.doi.org/10.1021/ic401666m | *Inorg. Chem.* 2013, 52, 10632−10642

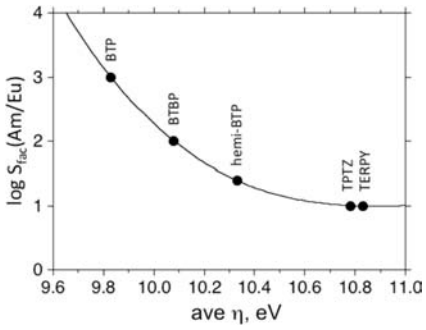

Figure 15. Plot of the log S_{fac}(Am/Eu) values (see Figure 16 in ref 3) versus ave η (Table 4).

The relationship in Figure 15 suggests that the observed An/Ln selectivity reflects the hardness of individual donor groups present in the extractant. Given that **7** is only slightly softer than **1**, this relationship correctly predicts that S_{fac}(Am/Eu) for TPTZ is about the same as that for TERPY. Given that **6** is the softest azine and **1** is the hardest azine, this relationship also predicts the observed increase in S_{fac}(Am/Eu) as the percentage of **6** increases relative to **1**; in other words, BTP > BTBP > hemi-BTP > TERPY. Finally, given that **2** is the second softest azine donor, this relationship predicts that polyazines containing **2** should also provide high An/Ln selectivity factors. Combining the ave η values in Table 4 with the correlation in Figure 15 predicts S_{fac}(Am/Eu) values of 140 for **2**-**1**-**2**, 2300 for **2**-**4**-**2**, and 200 for **2**-**7**-**2**.

SUMMARY

The results have shown that the behavior of polyazine ligands can be rationalized by the properties of individual azines and bisazine chelates. For example, TERPY (**1**-**1**-**1**), hemi-BTP (**1**-**1**-**6**), and BTP (**6**-**1**-**6**) all contain azines that form some of the strongest metal−nitrogen interactions, **1** and **6**. Thus, these extractants exhibit some of the strongest metal-ion affinities that can be obtained by connecting simple azines together in this architecture. By substituting the strongly basic **1** with the acidic **6**, one obtains ligands that function under increasingly acidic conditions, as illustrated by the series TERPY, hemi-BTP, and BTP. The same series of extractants also illustrates that, as the hardest azine, **1**, is replaced with the softest azine, **6**, the An/Ln selectivity is increased.

The criteria developed in this study provide a paradigm needed to address the question as to whether other viable trisazine extractants can be achieved by variation of the azine donor composition within the TERPY architecture. The answer is yes. Pyridazine, **2**, has the strongest intrinsic affinity for metal ions and is the second softest donor. Using this information, it is possible to identify three new prototype azine compositions that should exhibit properties desirable for application in An/Ln separations: high metal-ion affinity and An/Ln selectivity. These are **2**-**1**-**2**, **2**-**4**-**2**, and **2**-**7**-**2**, as well as the preorganized analogues **2**-**1**-**2**,p and **2**-**4**-**2**,p. The latter exhibit the highest metal-ion affinities that can be achieved when three simple azine donors are preorganized in this configuration.

This study has focused solely on the properties of simple azines and how variation in the azine donor composition influences metal complexation by polyazines. Although the results provide a framework for understanding why existing ligands work and guiding the design of new ligands, it is important to recognize that identification of a novel azine donor composition represents only the first step toward the development of a functional extractant. Many other factors must be addressed including the solubility of both the ligand and metal complex in the organic phase, chemical stability, radiolytic stability, ease of synthesis, and cost. As emphasized in prior reviews,[3−7] much effort has been expended to identify lipophilic substitution that yields optimal behavior under actual process conditions. During this optimization process, application of the methods presented herein should prove useful in understanding and predicting the influence of adding alkyl, aryl, and/or other substituents on properties such as the metal-ion affinity, basicity, and hardness.

ASSOCIATED CONTENT

Supporting Information

Optimized atomic coordinates and absolute energies for **1**−**7**, bisazines, trisazines, and their La^{3+} complexes. This material is available free of charge via the Internet at http://pubs.acs.org.

AUTHOR INFORMATION

Corresponding Author

*E-mail: haybp@ornl.gov. Phone: (865) 574-6717. Fax: (865) 574-4939.

Notes

The authors declare no competing financial interest.

ACKNOWLEDGMENTS

This research was sponsored by the Fuel Cycle Research and Development Program, Office of Nuclear Energy, U.S. Department of Energy.

REFERENCES

(1) (a) Denniss, I. S.; Jeapes, A. P. In *The Nuclear Fuel Cycle*; Wilson, P. D., Ed.; Oxford University Press: Oxford, U.K., 1986; pp 116−132. (b) Nash, K. L.; Choppin, G. R. *Sep. Sci. Technol.* **1997**, *32*, 255−274.

(2) Nash, K. L.; Madic, C.; Mathur, J. N.; Lacquement, J. In *The Chemistry of the Actinide and Transactinide Elements*, 3rd ed.; Morss, L. R., Edelstein, N. M., Fuger, J., Katz, J. J., Eds.; Springer: Dordrecht, The Netherlands, 2006; Vol. *4*, pp 2622−2798.

(3) Ekberg, C.; Fermvik, A.; Retegan, T.; Skarnemark, G.; Foreman, M. R. S.; Hudson, J. J.; Englund, S.; Nilsson, M. *Radiochim. Acta* **2007**, *95*, 637−642.

(4) Kolarik, Z. *Chem. Rev.* **2008**, *108*, 4208−4252.

(5) Lewis, F. W.; Hudson, M. J.; Harwood, L. M. *Synlett* **2011**, *18*, 2609−2632.

(6) Panak, P. J.; Geist, A. *Chem. Rev.* **2013**, *113*, 1199−1236.

(7) Hudson, M. J.; Harwood, L. M.; Laventine, D. M.; Lewis, F. W. *Inorg. Chem.* **2013**, *52*, 3414−3428.

(8) (a) Musikas, C., Le Marois, G., Fitoussi, R., Cuillerdier, C., Navratil, J. D., Schulz, W. W., Eds. *Properties and Uses of Nitrogen and Sulfur Donors Ligands in Actinide*; ACS Symposium Series 117; American Chemical Society: Washington, DC, 1980. (b) Musikas, C.; Vitorge, P.; Pattee, D. *Proceedings of the International Solvent Extraction Conference (ISEC 1983)*, Denver, CO, Aug 26−Sept 2, 1983; Metallurgical Society of AIME: Pittsburgh, PA, 1983.

(9) Hancock, R. D.; Martell, A. E. *Chem. Rev.* **1989**, *89*, 1875−1914.

(10) (a) Hay, B. P.; Zhang, D.; Rustad, J. R. *Inorg. Chem.* **1996**, *35*, 2650−2658. (b) Hay, B. P.; Hancock, R. D. *Coord. Chem. Rev.* **2001**, *212*, 61−78. (c) Hay, B. P.; Oliferenko, A. A.; Uddin, J.; Zhang, C.; Firman, T. K. *J. Am. Chem. Soc.* **2005**, *127*, 17043−17053.

(11) Frisch, M. J.; Trucks, G. W.; Schlegel, H. B.; Scuseria, G. E.; Robb, M. A.; Cheeseman, J. R.; Scalmani, G.; Barone, V.; Mennucci, B.; Petersson, G. A.; Nakatsuji, H.; Caricato, M.; Li, X.; Hratchian, H. P.; Izmaylov, A. F.; Bloino, J.; Zheng, G.; Sonnenberg, J. L.; Hada, M.; Ehara, M.; Toyota, K.; Fukuda, R.; Hasegawa, J.; Ishida, M.; Nakajima,

T.; Honda, Y.; Kitao, O.; Nakai, H.; Vreven, T.; Montgomery, J. A., Jr.; Peralta, J. E.; Ogliaro, F.; Bearpark, M.; Heyd, J. J.; Brothers, E.; Kudin, K. N.; Staroverov, V. N.; Kobayashi, R.; Normand, J.; Raghavachari, K.; Rendell, A.; Burant, J. C.; Iyengar, S. S.; Tomasi, J.; Cossi, M.; Rega, N.; Millam, N. J.; Klene, M.; Knox, J. E.; Cross, J. B.; Bakken, V.; Adamo, C.; Jaramillo, J.; Gomperts, R.; Stratmann, R. E.; Yazyev, O.; Austin, A. J.; Cammi, R.; Pomelli, C.; Ochterski, J. W.; Martin, R. L.; Morokuma, K.; Zakrzewski, V. G.; Voth, G. A.; Salvador, P.; Dannenberg, J. J.; Dapprich, S.; Daniels, A. D.; Farkas, Ö.; Foresman, J. B.; Ortiz, J. V.; Cioslowski, J.; Fox, D. J. *Gaussian 09*, revision A.2; Gaussian, Inc.: Wallingford, CT, 2009.

(12) (a) Becke, A. D. *J. Chem. Phys.* **1993**, *98*, 5648−5652. (b) Lee, C.; Yang, W.; Parr, R. G. *Phys. Rev. B: Condens. Matter* **1988**, *37*, 785−789.

(13) (a) Hay, P. J.; Wadt, W. R. *J. Chem. Phys.* **1985**, *82*, 270−283. (b) Hay, P. J.; Wadt, W. R. *J. Chem. Phys.* **1985**, *82*, 299−310. (c) Wadt, W. R.; Hay, P. J. *J. Chem. Phys.* **1985**, *82*, 284−298.

(14) Bacskay, G. B. *Chem. Phys.* **1981**, *61*, 385−404.

(15) *Spartan'10*, version 1.1.0; Wavefunction, Inc.: Irvine, CA, 2011.

(16) Zhan, C.-G.; Nichols, J. A.; Dixon, D. A. *J. Phys. Chem.* **2003**, *107*, 4184−4195.

(17) Marenich, A. V.; Olson, R. M.; Kelly, C. P.; Cramer, C. J.; Truhlar, D. G. *J. Chem. Theory Comput.* **2007**, *3*, 2011−2033.

(18) Mehdoui, T.; Berthet, J.-C.; Thuery, P.; Ephritikhine, M. *Dalton Trans.* **2004**, 579−590.

(19) (a) Choppin, G. R. *J. Alloys Compd.* **2002**, *344*, 55−59. (b) Choppin, R. G. *Pure Appl. Chem.* **1971**, *27*, 23−42.

(20) Joule, J. A.; Mils, K. *Heterocyclic Chemistry*, 4th ed.; Blackwell Publishing: Oxford, U.K., 2000.

(21) Brink, T.; Murray, J. S.; Politzer, P. *J. Org. Chem.* **1991**, *56*, 2934−2936.

(22) Khabibulina, I. V.; Volovodenko, A. P.; Trifonov, R. E.; Yashukova, G. V.; Mochulskaya, N. N.; Charushin, V. N.; Rusinov, G. L.; Beresnev, D. G.; Itsikson, N. A.; Ostrovskii, V. A. *Chem. Heterocycl. Compd.* **2003**, *39*, 616−623.

(23) Heitzmann, M.; Bravard, F.; Gateau, C.; Boubais, N.; Berthon, C.; Pecaut, J.; Charbonnel, M.-C.; Delangle, P. *Inorg. Chem.* **2009**, *48*, 246−256.

(24) (a) *Cambridge Structural Database*, version 5.3.4; 2012. (b) Allen, F. H. *Acta Crystallogr.* **2002**, *B58*, 380−388.

(25) Shannon, R. D. *Acta Crystallogr.* **1976**, *A32*, 751−767.

(26) Hancock, R. D. *Chem. Soc. Rev.* **2013**, *42*, 1500−1524.

(27) (a) MM3 force field as implemented in *PCModel*, version 9.3; Serena Software: Bloomington, IN, 2011. (b) Allinger, N. L.; Yuh, Y. H.; Lii, J. H. *J. Am. Chem. Soc.* **1989**, *111*, 8551−8566. (c) Lii, J. H.; Allinger, N. L. *J. Am. Chem. Soc.* **1989**, *111*, 8566−8575. (d) Lii, J. H.; Allinger, N. L. *J. Am. Chem. Soc.* **1989**, *111*, 8576−8582.

(28) Hancock, R. D.; Nikolayenko, I. V. *J. Phys. Chem.* **2012**, *116*, 8572−8583.

(29) (a) Busch, D. H.; Farmery, K.; Goedken, V.; Katovic, V.; Melnyk, A. C.; Sperati, C. R.; Tokel, N. *Adv. Chem. Ser.* **1971**, *100*, 44−57. (b) McDougall, G. J.; Hancock, R. D.; Boeyens, J. C. A. *J. Chem. Soc., Dalton Trans.* **1978**, 1438−1444. (c) Anicini, A.; Fabbrizzi, L.; Paoletti, P.; Clay, R. M. *J. Chem. Soc., Dalton Trans.* **1978**, 577−583. (d) Cram, D. J.; Kaneda, T.; Helgeson, R. C.; Brown, S. B.; Knobler, C. B.; Maverick, E.; Trueblood, K. N. *J. Am. Chem. Soc.* **1985**, *107*, 3645−3657. (e) Stack, T. D. P.; Hou, Z. G.; Raymond, K. N. *J. Am. Chem. Soc.* **1993**, *115*, 6466−6467.

(30) Martell, A. E.; Smith, R. M. *Critcal Stability Constants*; Plenum Press: New York, 1974−1989; Vols. *1*−*6*.

(31) Carolan, A. N.; Mroz, A. E.; Ojaimi, M. E.; Van Derveer, D. G.; Thummel, R. P.; Hancock, R. D. *Inorg. Chem.* **2012**, *51*, 3007−3015.

(32) Lewis, F. W.; Harwood, L. M.; Hudson, M. J.; Drew, M. G. B.; Desreux, J. F.; Vidick, G.; Bouslimani, N.; Modolo, G.; Wilden, A.; Sypula, M.; Vu, T.-H.; Simonin, J.-P. *J. Am. Chem. Soc.* **2011**, *133*, 13093−13102.

(33) Lewis, F. W.; Harwood, L. M.; Hudson, M. J.; Drew, M. G. B.; Hubscher-Bruder, V.; Videva, V.; Arnaud-Neu, F.; Stamberg, K.; Vyas, S. *Inorg. Chem.* **2013**, *52*, 4993−5005.

(34) Lan, J.-H.; Shi, W.-Q.; Yuan, L.-Y.; Li, J.; Zhao, Y.-L.; Chai, Z.-F. *Coord. Chem. Rev.* **2012**, *256*, 1406−1417.